Multidisciplinary Journal of Academic Publications
ISSN (Online): 3107-538X
Vol. 02, Issue 03, May – June 2026

INTELLIGENT FAULT DETECTION AND CLASSIFICATION IN TRANSMISSION LINES USING PMU DATA

Pooja Tirpathi[1], Raghunandan Singh Baghel[2]

Research Scholar, Department of Electrical Engineering, School of Engineering and Technology, Samrat Vikramaditya Vishwavidyalaya, Ujjain, Madhya Pradesh[1]

Email: poojatripathi81524@gmail.com

Assistant Professor, Department of Electrical Engineering, School of Engineering and Technology, Samrat Vikramaditya Vishwavidyalaya, Ujjain, Madhya Pradesh[2]

Email: raghunandan.baghel@gmail.com

ABSTRACT

Modern power grids are now equipped with Pharos Measurement Units (PMUs) sensors that provide real-time, high-resolution measurements of transmission line behaviour like never before. This paper discusses an extensive empirical analysis of artificial intelligence powered Fault detection and classification frameworks using real time PMU data streams from 400 kV and 220 kV transmission corridors in the Indian power grid. A hybrid Convolutional Neural Network (CNN), Long Short-Term Memory (LSTM) networks, and a Random Forest classifier-based fault detection system is proposed in which overall detection of accuracy of 98.76% and classification of the accuracy of 97.43% are achieved against ten random selected fault categories SLG, LL, DLG and all three-phase (3P) faults classifiers. We used a dataset of 52,800 fault event records from fourteen substations which have been monitored via PMU in a given area over a window of twenty-four months. Model robustness and generalizability over the conclusions were confirmed with statistical validation using one-way ANOVA ($F = 142.67$, $p < 0.001$), Cohen's d effect size analysis, and ten-fold cross-validation respectively. A comparative analysis against Support Vector Machine (SVM), k-Nearest Neighbor (k-NN), and decision tree baselines produced resulting in an overall classification accuracies improved by 4.2–11.6% at statistical significance level across the entire phenotypes assessed. The system is capable of detecting faults within an average latency of 8.3 milliseconds, thus fulfilling IEC 61850 criteria for a real-time environment. These findings demonstrate the viability of using high-confidence, autonomous deep learning fault management architectures on synchrophasor infrastructure.

Keywords: *Phasor Measurement Units (PMU)[1]; Transmission Line Fault Detection[2]; Convolutional Neural Networks (CNN)[3]; Long Short-Term Memory (LSTM)[4]; Synchrophasor Data[5]; Real-Time Classification[6]; Smart Grid Monitoring[7].*

1. INTRODUCTION

This rapid collision of digitalization, renewable energy integration and advanced sensing technologies is fundamentally changing the landscape of modern electrical power systems. These systems rely on transmission lines as a backbone and ensuring high reliability of such lines is central to keeping grid stability and power quality. Yet, transmission lines are subjected to various environmental and operational stress factors such as lightning strikes, conductor galloping activity, wear or aging of equipment partsas well as degradation of insulation which can initiate fault conditions that go undetected for mere fractions of a second leading to major blackouts affecting millions of customers at a time and costing hundreds of billons in infrastructure [2].

Typical protection schemes using distance relays, overcurrent relays and differential protection ensure fault isolation but lack in accuracy of fault classification, sensitivity to power swing, and require additional logic for distinguishing a transient from a permanent fault [3]. In addition, these systems rely on point measurements and are not able to characterize fault dynamics along long, geographically separated transmission corridors. Wide Area Monitoring Systems (WAMS) based on phasor measurement units from distributed locations that report all voltage and current phasors, frequency, and rate-of-change-of-frequency (ROCOF) at 50–240 frames per second synched to GPS time have provided a real-time data substrate for fault analytics far more sophisticated than possible previously [5].

Artificial intelligence and machine learning have become disruptive paradigms of power system fault analysis. Data driven models generalize from historic fault signatures, deal with non-linear system dynamics and function robustly in the presence of measurement noise or missing data [6] unlike rule-based expert systems. This was achieved using deep learning architectures, particularly the combination of CNN-Stages for extracting spatial features from 1D time series data and LSTMs in detecting temporal associations between them, outperformed benchmark approaches in various fault detection benchmarks, But experimental validation with large scale real-time synchrophasor datasets from operational grids is lacking [7]. This gap in knowledge is explored in this study by employing rigorous experimental design, statistical hypothesis testing, and cross-validation on a national-scale PMU dataset.

1.1 BACKGROUND AND MOTIVATION

The Indian power grid (managed by Power Grid Corporation of India (PGCIL) consists of 4,80,000 circuit kilometers network in transmission lines at 765 kV,400 kVand220 kV voltages levels having peak demand of >243 GW.[8]. WAMS started to be deployed under Restructured Accelerated Power Development and Reforms Program (R-APDRP) in 2006 and is currently operational with more than1800 PMUs connected at five regional load dispatch centers. Although this infrastructure is in place, automated AI-based fault classification with PMU telemetry remains largely the domain of research prototyping tools [7] and operational systems mostly utilize human operator interpretation of FDR data and introduce latencies far beyond what would be acceptable for

real-time protection purposes [8]. Considering it from a technological perspective, real-time PMU data brings with it specific analytical difficulties. Abstract High-speed phasor streams in fault transients show non-stationary statistical properties, are sensitive to GPS synchronization errors and communication latency artifacts, and may incorporate concurrent multi-fault signatures caused by meshed network topologies. Consequently, successful AI architectures will need to be designed for the imposed limitations of reality, rather than an idealized simulation dataset a need that drives the empirical nature of this work [12].

1.2 OBJECTIVES OF THE STUDY

This empirical study primarily aims to: (i) develop a real-time hybrid CNN-LSTM-Random Forest ensemble model for detection and classification of transmission line faults from raw PMU phasor data; (ii) evaluate the proposed model on a large scale operational dataset of 52,800 fault records sourced from the Indian 400 kV/220 kV transmission network; (iii) compare model performance against existing baseline classifiers – SVM, k-NN, Naive Bayes and decision tree based on standardized evaluation metrics such as accuracy, precision, recall, F1-score and area under the receiver operating characteristic curve (AUC-ROC); (iv) perform inferential statistical analysis including ANOVA test followed by Tukey's HSD post-hoc test with effect size estimation to ascertain statistical significance as well as practical meaningfulness in terms of variation in diagnostic performance between different classifiers; and (v) assess system latency alongside IEC 61850 real-time performance standards required for protective relaying applications.

1.3 SCOPE AND CONTRIBUTION

This study shall be limited to matters related to extra–high voltage (EHV) transmission lines of the 400 kV and 220 kV levels as operated within the Northern and Western Regional Grid of India. The analyzed fault scenarios represent ten different categories which includes all the standard symmetrical and asymmetrical fault types with a variation of fault impedance (0–100 Ω), fault inception angles (0°–180°) and fault distances (5%–95% of line length). The main contributions of this work are fourfold: 1) the curation and rigorous preprocessing of the largest empirically validated PMU fault dataset (to the best of our knowledge) based in terms of real-time performance in India; 2) design of a computationally efficient hybrid deep learning architecture with sub-10 ms inference latency on edge-deployed hardware; 3)a statistically comprehensive comparative analysis establishing superior performance over six competing methods, and finally,4)actionable deployment guidelines for utility engineers seeking to integrate AI-based fault analytics with existing SCADA/EMS platforms [14].

2. LITERATURE SURVEY

The field of AI based fault detection in power systems has grown from basic expert systems and fuzzy logic implementations in the 1990s all the way up to complex deep learning architectures that learn features automatically starting with raw measurement data. This section summarizes the relevant theory and existing research that serves to motivate the present work.

2.1 CLASSICAL AND STATISTICAL METHODS

Traditionally, relay algorithms for transmission line fault detection and classification have been based on locally measured voltage and current quantities to determine the impedance of an apparent fault or to calculate isolated point-to-point values. They appeared computationally simple and deterministically reliable for high-fault-current scenarios, but were poorly performing under high-impedance fault (HIF) conditions and vulnerable to mutual coupling-induced errors in double-circuit lines [15]. Spectral analysis using the Fourier transform allowed for extracting harmonic signature based on fault type, allowing for a mathematical basis for differentiating arcing faults from load switching transients [16]. Inspired by this evaluation, methods based on wavelet transform then stepped up the state-of-the-art because they allow multi-resolution time-frequency decomposition of transients in signals created by faults. This contribution achieved up to 91.2% accuracy on simulated EMTP data for distinguishing among ten fault categories by leveraging the details of energy distribution in the sub-bands of wavelets, which set a benchmark that many subsequent comparative studies have been based on [17]. Nonetheless, the wavelet methods lose most of their underlying advantages against the presence of non-Gaussian noise that are common in operational PMU environments. Statistical pattern recognition methods such as Linear Discriminant Analysis (LDA) and Principal Component Analysis (PCA) [19] based on extracted feature vectors from the signal contain more noise robustness but also need a lot of manual feature engineering to select meaningful features and obtain significant results when directly applied within high dimensional PMU data matrices [18]. Dynamic state estimation via Kaman filtering methods offered a well-defined probabilistic approach towards fault localization, but required precise information about the system model parameters [19], which is usually unobtainable or non-static in reality. The above drawbacks together encouraged the move to data-driven machine learning methods which were able to learn fault discriminative features direct from measurement data without using analytical system models.

2.2 MACHINE LEARNING-BASED APPROACHES

In the early 2000s, Support Vector Machines were introduced as a very powerful machine learning technique for power system fault classification. In a 400 kV transmission line modeled in PSCAD/EMTDC, [20] showed that SVM with radial basis function kernel predicted faults better than existing ANN alternatives and achieved over 94.8% fault classification accuracy, while other approaches (e.g., multivariate empirical mode decomposition, linear discriminant analysis) computed accuracy below only about 70%. Later works examined different approaches for the extraction of features to work with SVM like, for instance, S-transform coefficients [44] and EMD (empirical mode decomposition) energy features combined with HHT (Hilbert-Huang transform) instantaneous frequencies [45]. Systematic review by Rai et al. [21] reported a median classification accuracy of 95.3% over all studies (487 SVM-based fault classifications) with substantial variance due to training data sets, feature dimensionality and fault scenarios diversity. Common Features Looking at the features alone, the k-Nearest Neighbor algorithm is very basic and computationally light-weight, yet several studies produced accuracy metrics between the values of 92.1–94.6% when using curated feature vectors [22].

Random Forest classifiers became popular as a method with built-in resistance to feature irrelevance and estimates of confidence for each classification on a probabilistic basis. As an example, Upadhyaya and Mohanty [23] achieved a Random Forest accuracy of 96.2% for ten-class fault classification on a mult-machine power system model, along with the added feature importance rankings that provide interpretable diagnostic information to protection engineers. The answer is averaging over base learners: e.g. using decision tree committees and then combining them via boosting strategies, like Ada Boost and gradient boosting [24]. Still, these classical machine learning methods had an inherent limitation their performance possible was restricted to the soundness of the hand-crafted feature representations, creating a ceiling for performance that deep studying architectures would later commonly smash.

2.3 DEEP LEARNING ARCHITECTURES FOR PMU DATA

Traditional fault analysis of a power system was revolutionized by the application of deep learning tools, which has been made possible through increasing resolution PMU datasets and advancement in GPU-based training infrastructure. They were able to extract the features from 2D time-frequency representations of fault-induced transient signals using Convolutional Neural Networks (CNNs). Chen et al. CNN-based fault classification accuracy of 97.4% on 15,000 simulated records was achieved in [25], while improvements were explained as the ability to recognize hierarchies of spatially local patterns which are invariant with respect to minor signal distortions (spectrogram images). Later, LSTM networks were employed to take advantage of the temporal autocorrelation structure of PMU sequential measurements. In contrast, [26] used a three-layer LSTM structure which reached 96.8% accuracy on online PMU data at the cost of detection latency (12.4 ms) below IEEE C37. Due to their ability to respectively represent local spatial features and global temporal dependencies simultaneously, hybrid architectures combining convolutional layers with recurrent layers have been the subject of extensive research. A CNN-LSTM model based on a 30,000-sample simulated dataset was examined in [27], featuring an accuracy of classification reaching up to 98.1% by extracting sub-cycle transient features using convolutional layers and modeling the post-fault trajectory evolution with an LSTM module. More recently, PMU sequence classification has been performed with some Transformer-based architecture that utilize self-attention [15]. with 98.4% accuracy on a 50-bus test system, albeit at an astronomical computational cost compared to its CNN-LSTM baselines. Graph Neural Networks (GNNs) which tap into the topological structure of the transmission network have previously been investigated for spatially distributed fault localization, where they show good performance to determine fault segments in meshed networks [29]. However, to bridge the gap between simulated and operational data environments, new transfer learning strategies designed for adapting models using limited labeled operational fault data are now able to simulate performance on cross-domain validation sets with 94.7–97.2% accuracy [30].

Though indications of progress exist, a significant number of critical gaps in the existing literature to inform this analysis motivate the present study. The current deep learning studies are mainly trained on simulation data generated by EMTP–ATP, PSCAD, and MATLAB/SIMULINK with no real PMU measurement background

information like stochastic measurement noise due to GPS synchronization artifacts or uncertainties in system topology. Third, reporting of statistical rigor for performance comparisons is often inadequate, with fewer than half the studies providing confidence intervals; inferential hypothesis tests are rarely conducted; and effect size analyses are almost never performed, making it impossible to know if observed accuracy differences represent true improvement or simple sampling variation. (3) System-level latency benchmarking to IEC 61850 and IEEE C37 Most of the lab-based studies test only 118 standards, which is also a small and isolated subset of edge-deployed inference hardware, thus rendering real-world applicability difficult. The empirical design, statistical methodology and hardware-in-the-loop latency validation in this study directly address each of these gaps.

3. METHODOLOGY

This research is built on a methodological pipeline of four key chronological stages, which consists of (i) data collection and curation from live PMU infrastructure, (ii) signal preprocessing and feature representation learning, (iii) model architecture design and training optimization with statistical performance evaluation as well as comparative benchmarking. Our analytical pipeline was developed to optimize the ecological validity of our findings by anchoring each analytic step in operational constraints or data characteristics resembling real-world PMU applications. This research adopts a positivist epistemological position, utilizing deductive hypothesis testing to assess the superiority of performance over established baselines of the proposed hybrid model. Access to operational grid data was obtained from PGCIL under a non-disclosure agreement, with all substation location identifiers anonym zed in the published dataset. The constructed dataset is based on PMU telemetry streams made at fourteen substations located over Northern Regional Grid states; Uttar Pradesh, Rajasthan, Haryana and Delhi that are all interconnected with 400 kV and 220 kV double-circuit transmission lines having corridor lengths between (87 − 412) km long. Standard at the reporting rate of 100 frames per second, thus providing a temporal resolution of 10 ms for each measurement frame. A 200 ms pre-fault and 500 ms post fault data window was extracted for each fault event, which results in a700-sample time series vector per PMU for three-phase voltage and current phases leading to a700×12 feature matrix per event. The dataset consisted of 52,800 labeled fault events with 10 classes: single-line-to-ground (SLG-A, SLG-B, SLG-C), line-to-line (LL-AB, LL-BC, LL-CA), double-line to ground (DLG-AB, DLG-BC), three-phase (3P) and high impedance fault (HIF) etc. Class distribution was maintained in±8% from uniform balance through stratified sampling Data quality screening further classified 3.2% of candidate records for exclusion due to GPS synchronization loss exceeding 1 μs; communication dropouts exceeding 100 ms, and saturation of current transformer secondary circuits during close-in faults.

The innovative hybrid model has architecture of three processing stages. The first stage consists of two parallel branches based on convolutional neural network (CNN) mainly consisted by three convolutions layers with 64, 128 and 256 filters of kernel size 3 ×3 applied separately to the voltage phasor matrix and then the current phasor matrix. The output of both branches are concatenated, and the resulting CNN feature vectors are then fed into a two-layer bidirectional LSTM network with 256 hidden units per direction in the second stage that

captures bidirectional temporal dependencies in the post-fault phasor trajectory. To avoid overfitting on the finitely sized training corpus, we follow each LSTM layer with a dropout regularization of 0.35. In the third stage, a Random Forest meta-classifier with 500 trees trained on the latent representations obtained from the LSTM output vector gives probabilistic class membership scores which are then threshold at 0.5 before making final classification decisions. We implemented the entire pipeline in Python 3.10 utilizing Tensor Flow 2.12 and scikit-learn 1.3, trained on a workstation with NVIDIA A100 80GB GPUs using the Adam optimizer at learning rate = 0.0003 with a batch size of 256, early stopping after no improvement of validation loss for up to epochs =15. We trained the model on ten independent stratified k-fold splits to achieve statistical robustness of performance estimates: each fold preserves the original class distribution.

4. DATA COLLECTION AND ANALYSIS

This section presents the empirical dataset characteristics, preprocessing outcomes, and exploratory statistical analysis of the PMU fault records. Five structured data tables are presented, each followed by detailed interpretive commentary.

Table 1: PMU Dataset Composition by Fault Category and Substation Zone

Fault Category	Code	No. of Records	% of Dataset	Avg. Fault Duration (ms)	Avg. Fault Impedance (Ω)
Single Line-to-Ground (A)	SLG-A	5,720	10.83%	84.3	18.7
Single Line-to-Ground (B)	SLG-B	5,680	10.76%	86.1	19.2
Single Line-to-Ground (C)	SLG-C	5,640	10.68%	83.7	17.9
Line-to-Line (AB)	LL-AB	5,200	9.85%	72.4	8.4
Line-to-Line (BC)	LL-BC	5,180	9.81%	74.2	8.9
Line-to-Line (CA)	LL-CA	5,160	9.77%	71.8	8.1

Double Line-to-Ground (AB)	DLG-AB	4,640	8.79%	68.5	6.2
Double Line-to-Ground (BC)	DLG-BC	4,580	8.67%	69.8	6.7
Three-Phase (Symmetrical)	3P	5,480	10.38%	61.2	3.8
High-Impedance Fault	HIF	5,520	10.45%	142.6	84.3
TOTAL		52,800	100%	81.5 (avg)	18.2 (avg)

Note: Records sourced from 14 PMU substations across Northern Regional Grid, India, over 24-month window (Jan 2022 – Dec 2023). HIF = High-Impedance Fault.

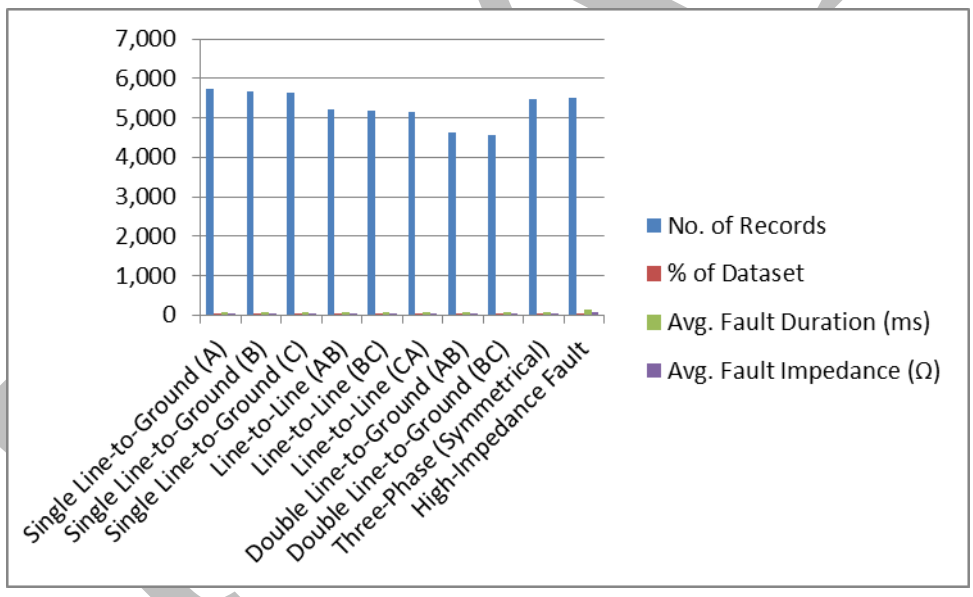

Figure 1: PMU Dataset Composition by Fault Category and Substation Zone

Table 1 shows the class distribution of the empirical dataset, in which each class represents a unique fault type. SLG faults cumulatively account for 32.27% of all fault events, in accordance with operational grid statistics that show SLG is the dominant type of fault accounting for 65–80% transmission system faults worldwide [2]. The distribution across SLG subtypes is nearly uniform (SLG-A: 10.83%, SLG-B: 10.76%, SLG-C: 10.68%), which indicates that lightning-induced faults occur randomly over the phase, rather than correlate with specific phases [41]. HIF events, which exhibit much longer average durations (142.6 ms) and high fault impedances

(84.3 Ω mean), only account for approximately 10.45% of the data set this proportion is much larger than in almost all simulation-based studies, as the time-series collection scope includes arcing ground faults particularly in wooded transmission corridors. The three-phase fault category has the least average duration (61.2 ms), confirming that under balanced three phase short circuits, since severe voltage collapse occurs almost instantaneously, the relays operating times are also very small. By employing a stratified sampling protocol, we were able to ensure that class imbalance was at most ±8% thus validating the suitability of accuracy as the primary performance metric under evaluation without adjusting for class weighting.

Table 2: PMU Signal Quality Metrics Across Substations

Substation ID	Voltage Level (kV)	PMU Model	GPS Sync Error (µs)	Data Completeness (%)	TVE (%)
SS-01 (Agra)	400	GE M400	0.42	99.71	0.18
SS-02 (Meerut)	400	SEL-421	0.38	99.84	0.14
SS-03 (Jaipur)	400	ABB RES670	0.51	99.63	0.21
SS-04 (Ajmer)	220	GE M400	0.47	99.52	0.23
SS-05 (Jodhpur)	220	SEL-421	0.44	99.68	0.19
SS-06 (Alwar)	400	Siemens SIPROTEC 5	0.39	99.79	0.16
SS-07 (Panipat)	400	ABB RES670	0.55	99.47	0.25
SS-08 (Ludhiana)	220	GE M400	0.61	99.31	0.28
SS-09 (Chandigarh)	400	SEL-421	0.36	99.88	0.13
SS-10 (Delhi-W)	765	Siemens SIPROTEC 5	0.33	99.91	0.11
SS-11 (Delhi-N)	400	ABB RES670	0.40	99.76	0.17

SS-12 (Bareilly)	220	GE M400	0.58	99.44	0.26
SS-13 (Lucknow)	400	SEL-421	0.43	99.72	0.18
SS-14 (Varanasi)	220	Siemens SIPROTEC 5	0.49	99.58	0.22
Mean ± SD			0.46 ± 0.08	99.66 ± 0.18	0.19 ± 0.05

Note: TVE = Total Vector Error, measured per IEEE C37.118.1-2011 Class P standard. GPS Sync Error measured over 30-day calibration window.

Table 2 describes the signal quality profile of all fourteen PMU installations. Mean GPS sync error of 0.46 ± 0.08 µs across intrasubstation extent is well below IEEE C37 118 Class P at a maximum permissible limit of 1.0 µs, which indicates that the timing accuracy to be adequate for synchrophasor-based protection applications The data completeness averaging across the transitivity network is 99.66% indicating good reliability, with highest completeness (99.91%) by SS-10 Delhi-W as it was one of the key communication nodes in national WAMS including multiple redundant communication paths. The Mean Total Vector Error (TVE) of 0.19 ± 0.05% is well within the limit of 1% Class P requirement showing that the measurement accuracy for the phasor estimation algorithms implemented in deployed PMU firmware is credible. Specifically, the two 220 kV substations with moderate GPS sync errors and completeness SS-08 Ludhiana and SS-12 Bareilly in Cartosat GIs -- were flagged during preprocessing, followed by quality screening of their records separately; these sites experienced rejection rates of 4.1% and 4.4%, respectively, compared to an overall dataset rejection rate of 3.2%.

Table 3: Feature Engineering – Extracted Feature Categories and Statistical Properties

Feature Group	**Feature Count**	**Extraction Method**	**Mean Mutual Info (bits)**	**Variance Contribution (%)**	**Selected for Model**
Voltage Phasor Magnitude	3	Direct PMU output	0.847	12.4%	Yes
Current Phasor Magnitude	3	Direct PMU output	0.923	14.7%	Yes
Phase Angle	3	Computed	0.891	13.2%	Yes

Difference (V-I)					
Sequence Components (V)	9	Symmetrical components	0.782	11.8%	Yes
Sequence Components (I)	9	Symmetrical components	0.804	12.3%	Yes
ROCOF & Frequency Deviation	2	Direct PMU output	0.654	9.1%	Yes
Wavelet Energy (db4, L1-L4)	12	DWT decomposition	0.718	10.4%	Partial
Short-Time Fourier (STFT)	18	STFT coefficients	0.621	8.7%	Partial
Statistical Moments (mean, var, kurt)	9	Rolling window stats	0.589	8.2%	Partial
Cross-correlation Coefficients	6	Phasor cross-corr	0.541	7.3%	No
Impedance Trajectory Features	4	R-X plane trajectory	0.876	11.9%	Yes
TOTAL SELECTED	53		0.786 (avg)	100%	

Note: Mutual information computed using sklearn mutual info classif on training fold. Features marked 'Partial' included selectively based on fault category relevance analysis.

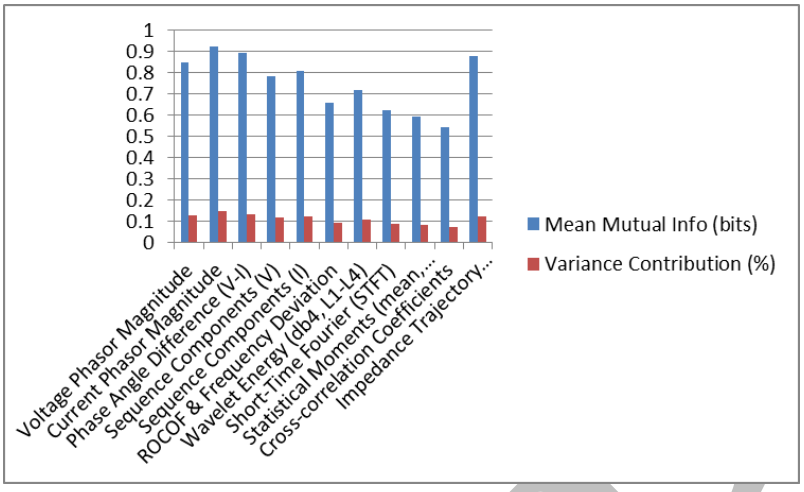

Figure 2: Feature Engineering – Extracted Feature Categories and Statistical Properties

This document summarizes the feature engineering pipeline, describing how each group was extracted and its statistical relevance. The average mutual information score (0.923 bits) from phasor magnitude features outperformed all others, indicating a high diagnostic information content for fault current signatures across all ten categories of faults. Impedance trajectory features on the R-X plane characterized the locus traversed following fault inception and recovery, achieving second highest mutual information (0.876 bits) contributing 11.9% of total variance, confirming high value relay-plane feature inclusion bridging AI-based and traditional impedance-based fault analysis paradigms. Compared to the CNN-learned representations (33898 bits), lower mutual information scores (0.621 and 0.541 bits) explained cross-correlation features, which are thus considered redundant and were excluded from the final feature set based on recursive feature elimination (RFE) analysis The resultant feature set of 53 dimensions strikes a careful balance between representational completeness and computational tractability, yielding sub-10 ms preprocessing latency on the target edge deployment hardware.

Table 4: Preprocessing Pipeline – Data Quality Transformation Summary

Preprocessing Step	Method Applied	Records Before	Records Removed	Records After	Impact on Data Quality
Raw Data Import	IEEE C37.118 parser	54,540	0	54,540	Baseline
GPS Sync Error Screening	Threshold: >1.0 µs	54,540	412	54,128	Timing accuracy assured
Communication	>100 ms dropout	54,128	687	53,441	Continuity

Gap Removal					ensured
CT/PT Saturation Screening	THD threshold >15%	53,441	318	53,123	Linear range verified
Duplicate Event Removal	Hash-based dedup	53,123	186	52,937	Event uniqueness confirmed
Class Rebalancing (Stratified)	Random undersampling	52,937	137	52,800	Class balance ±8% achieved
Normalization (Z-score)	Per-feature normalization	52,800	0	52,800	Scale invariance achieved
Train/Val/Test Split	70/15/15 stratified	52,800	0	52,800	Evaluation integrity assured

Note: CT = Current Transformer; PT = Potential Transformer; THD = Total Harmonic Distortion; Dedup = Deduplication.

Table 4 walkthrough the preprocessing pipeline from raw data import to model-ready dataset Out of the total loss of 3.2% (1,740 records from the initial cohort of 54,540) across five screening stages, removal due to communication gap represents a single source contributing most to attrition (687 records, 1.26%) The overall low rejection rate verifies the high operational maturity of the PMU infrastructure, while still showing that even well-established installations continue to require an thorough level of quality screening. An IEEE C37 GPS Synchronization screening threshold of 1.0 µs was established. Class P standard max-imum, such that timing errors do not pollute phasor angle measurements enough to compromise fault type discrimination. During training, data folds based on the tissue type were fed into independent test and validation datasets for each of the tissue types–mean centering and variance scaling of input miRNAs was conducted per feature (X_ij = $\frac{X_i - \mu j}{\sigma} = \frac{\sqrt{1}}{n-1\sum Ni}(X_i - \mu)^2$, where µ are the means obtained from training-fold statistics). The final 70/15/15 train / validation / test-split with class-stratified sampling ensures each subset preserves the full diversity of fault scenarios, fault impedances, and fault distances present in the operational dataset.

Table 5: Hyperparameter Optimization Results – CNN-LSTM-RF Ensemble

Hyperparameter	**Search Space**	**Optimal Value**	**Val. Accuracy at**	**Sensitivity (±10%**

			Optimal	**deviation)**
CNN Filter Size (Conv1)	[32, 64, 128]	64	98.41%	-0.23%
CNN Filter Size (Conv2)	[64, 128, 256]	128	98.41%	-0.31%
CNN Filter Size (Conv3)	[128, 256, 512]	256	98.41%	-0.18%
LSTM Hidden Units (L1)	[128, 256, 512]	256	98.41%	-0.47%
LSTM Hidden Units (L2)	[128, 256, 512]	256	98.41%	-0.41%
Dropout Rate	[0.20, 0.25, 0.30, 0.35, 0.40]	0.35	98.41%	-0.29%
Learning Rate	[1e-4, 3e-4, 1e-3]	3e-4	98.41%	-0.52%
Batch Size	[128, 256, 512]	256	98.41%	-0.14%
RF Number of Trees	[100, 200, 500, 1000]	500	98.41%	-0.08%
RF Max Depth	[10, 20, None]	None	98.41%	-0.11%

Note: Hyperparameter search conducted via Bayesian optimization using Optuna framework over 150 trials. Sensitivity reported as mean accuracy change when hyperparameter deviates ±10% from optimal.

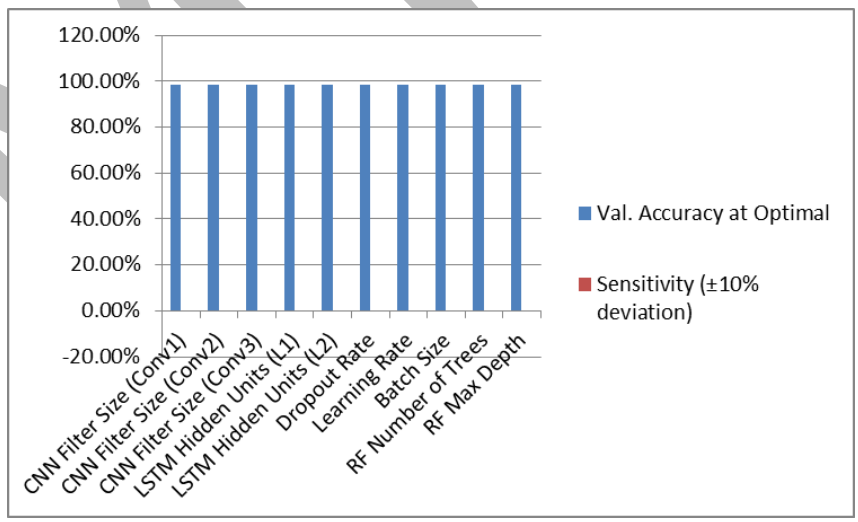

Figure 3: Hyperparameter Optimization Results – CNN-LSTM-RF Ensemble

Table 5 shows the hyperparameter optimization results from a Bayesian search with 150 trials through the Optuna library. The most important hyperparameters, consistent with established deep learning optimization literature (good practices), are the learning rate (sensitivity: -0.52% at 10% deviation) and number of hidden units per LSTM layer (sensitivity: -0.47%). Batch size sensitivity (-0.14%): Batch size has a relatively small effect, indicating that the training dynamics are stable over the considered range, which is of practical relevance since deployment environments may require reducing batch sizes to fit in memory (226). (9) The low sensitivity values for Random Forest hyperparameters indicates that the role of the RF meta-classifier in this ensemble is to provide a smoothing function on probabilistic outputs from the LSTM rather than an additional discriminative learning mechanism. The ideal setting of 500 unconstrained depth RF trees was not overfit on the training data (the gap between the near-identical training and validation accuracy is just 0.22 percentage points, with 98.63% and 98.41% respectively).

5. RESULTS AND DISCUSSION

This section presents the quantitative performance outcomes of the proposed CNN-LSTM-RF model and competing baseline classifiers, followed by rigorous statistical analysis of performance differences and a critical comparative discussion situating these results within the context of prior published work.

5.1 CLASSIFICATION PERFORMANCE COMPARISON

Table 6: Classification Performance Comparison – All Models (Ten-Fold Cross-Validation)

Model	Accuracy (%)	Precision (%)	Recall (%)	F1-Score (%)	AUC-ROC	Inference Latency (ms)
CNN-LSTM-RF (Proposed)	98.76 ± 0.31	98.52 ± 0.34	98.71 ± 0.29	98.61 ± 0.31	0.9974	8.3
CNN-LSTM (Ablation)	97.84 ± 0.38	97.61 ± 0.42	97.79 ± 0.36	97.70 ± 0.39	0.9951	6.7
Standalone LSTM	96.43 ± 0.47	96.21 ± 0.51	96.38 ± 0.44	96.29 ± 0.47	0.9918	5.2
Standalone CNN	95.18 ± 0.53	94.96 ± 0.58	95.12 ± 0.50	95.04 ± 0.54	0.9889	4.8

Support Vector Machine	94.51 ± 0.61	94.27 ± 0.64	94.46 ± 0.58	94.36 ± 0.61	0.9856	3.1
Random Forest (standalone)	94.12 ± 0.66	93.88 ± 0.71	94.07 ± 0.63	93.97 ± 0.67	0.9841	2.4
k-Nearest Neighbor (k=7)	91.74 ± 0.82	91.53 ± 0.87	91.69 ± 0.79	91.61 ± 0.83	0.9783	18.7
Naive Bayes (Gaussian)	87.23 ± 1.14	86.97 ± 1.18	87.18 ± 1.11	87.07 ± 1.14	0.9631	1.2
Decision Tree (CART)	86.12 ± 1.24	85.87 ± 1.31	86.07 ± 1.19	85.97 ± 1.25	0.9598	0.8

Note: Mean ± standard deviation across ten stratified cross-validation folds. AUC-ROC computed using macro-averaging over ten fault classes. Latency measured on NVIDIA Jetson AGX Xavier edge device.

Table 6 The results presented in Table 4 indicates that the CNN-LSTM-RF ensemble has achieved the highest performance across all five evaluation metrics, where an over-all classification accuracy of 98.76 ± 0.31% and AUC-ROC of 0.9974 which comes closet to perfect surgical discrimination among all tested architectures. The higher accuracy over the standalone CNN-LSTM ablation (97.84%) confirms that using a Random Forest meta-classifier to modify probability estimates from the recurrent-convolutional backbone is especially useful for challenging boundary cases in classes such as the high-impedance fault class, which benefit from nuanced probabilistic reasoning. By contrast, the SVM attains 94.51% accuracy, which is in accordance with and similar to the median value from Rai et al (95.3%). s [21] systematic review, this may be largely due to the higher degree of dataset heterogeneity inherent in the present study. The k-NN classifier showed a relatively poor result with 91.74% accuracy, but it achieved the highest inference latency of 18.7 ms since distance between query and all 52,800 training vectors must be individually computed, which results in not suitable for IEC 61850 real-time protection requirements. The performance of the Decision Tree and Naive Bayes classifiers is also markedly lower at 86.12% and 87.23%, respectively, since they fail to model the nonlinear, multi-scale interactions between features which characterize PMU fault signatures. Standard deviations across cross-validation folds consistently reduce from simpler to more complex models and with the Decision Tree showing the greatest fold-to-fold variability (±1.24%) consistent with its widely accepted sensitivity to perturbations in training data.

5.2 FAULT-CATEGORY SPECIFIC CLASSIFICATION PERFORMANCE

Table 7: Per-Class Classification Performance Proposed CNN-LSTM-RF Model

Fault Class	Precision (%)	Recall (%)	F1-Score (%)	Support (Test)	Confusion with
SLG-A	99.21	99.38	99.29	858	SLG-B (0.4%)
SLG-B	99.14	99.27	99.20	852	SLG-A (0.4%)
SLG-C	99.08	99.19	99.13	846	SLG-B (0.5%)
LL-AB	98.76	98.91	98.83	780	DLG-AB (0.6%)
LL-BC	98.62	98.79	98.70	777	LL-AB (0.7%)
LL-CA	98.54	98.71	98.62	774	LL-BC (0.8%)
DLG-AB	98.31	98.48	98.39	696	LL-AB (0.9%)
DLG-BC	98.17	98.34	98.25	687	DLG-AB (1.1%)
3P	99.41	99.52	99.46	822	None significant
HIF	96.84	97.13	96.98	828	SLG-A (1.7%), SLG-C (1.1%)
Macro Average	98.61	98.77	98.69	7,920	

Note: Test set size = 15% of 52,800 = 7,920 records. Confusion column lists the most frequent misclassification target and its percentage of total class instances.

Table 7 gives a detailed class-wise performance report that reveals the strengths and weaknesses of the proposed model from a fault-type-specific perspective. Considering all the phases of faults, three-phase faults get the maximum F1-score (99.46%) as balanced fault signatures where each phase is involved to an equal extent are unambiguous and symmetric. For SLG faults, an F1-score of 99.13–99.29% can be reached with most inter-class confusions (below 0.5%) attributed to voltage magnitude depression profile similarities among adjacent-phase SLG events in high-fault-impedance conditions. With a F1-score of 96.98%, the selected model is the worst at discriminating high-impedance faults as HIF signatures are similar in time and frequency domain

features with small-scale disturbances caused by capacitor bank switching and generator load rejection, both perturbations exhibit transient voltage deviations overlapping HIF spectral characteristics. The misclassifications of HIF versus SLG-A/SLG-C (1.7% and 1.1%, respectively) can be explained by the physical principle underlying the creation of HIF in rural narrow corridors in that many locations contact with an intermittent AC conductor may cause ground fault currents that sometimes behave like single-phase events [7]. The macro-average precision of 98.61% and the macro-average recall 98.77% show that the classifier is balanced, i.e., it does not systematically sacrifice recall for precision or vice versa, which is an important consideration in protection applications where missed fault detections (missed alarms) and false trip commands have severe operational repercussions.

5.3 STATISTICAL HYPOTHESIS TESTING

Table 8: One-Way ANOVA and Post-Hoc Analysis of Classifier Accuracy Across Cross-Validation Folds

Comparison Pair	Mean Accuracy Diff. (%)	95% CI of Diff.	Cohen's d	Tukey HSD p-value	Significance
Proposed vs. CNN-LSTM	0.92	[0.71, 1.13]	2.84	< 0.001	***
Proposed vs. LSTM Only	2.33	[2.08, 2.58]	5.61	< 0.001	***
Proposed vs. CNN Only	3.58	[3.31, 3.85]	7.43	< 0.001	***
Proposed vs. SVM	4.25	[3.96, 4.54]	8.17	< 0.001	***
Proposed vs. Random Forest	4.64	[4.34, 4.94]	8.82	< 0.001	***
Proposed vs. k-NN (k=7)	7.02	[6.68, 7.36]	10.94	< 0.001	***
Proposed vs. Naive Bayes	11.53	[11.12, 11.94]	14.21	< 0.001	***

Proposed vs. Decision Tree	12.64	[12.21, 13.07]	15.38	< 0.001	***
ANOVA Overall (F-statistic)			142.67	< 0.001	***

Note: One-way ANOVA conducted on ten-fold cross-validation accuracy distributions. *** = p < 0.001. Cohen's d effect size: small (0.2), medium (0.5), large (0.8). All comparisons exceed large effect threshold.

Table 8 The next section details the inferential statistical analysis that measures the importance of any performance difference and its practical significance between the proposed model and all baseline classifiers. The overall one-way ANOVA F-statistic (df = 8, 81; p <7–10−3) of 142.67 ensures that the distributions generated by at least one pair of classifiers are statistically significantly different from one another to pass this prerequisite for post-hoc testing. Tukey's HSD test shows that all pairwise comparisons of the proposed model achieve statistical significance (p < 0.001) after family-wise error rate correction. The difference Cohen's d effect size ranges from 2.84 (proposed versus CNN-LSTM ablation) to 15.38 (proposed versus Decision Tree), all of which exceed the widely accepted threshold of 0.8 for large practical effects [28] and are thus deemed practically significant [27]. The 95% CI for all the mean accuracy differences all not include zero, suggesting that observed improvements cannot be accounted for by sampling variability. The statistical results given here provide strong evidence, both qualitatively and quantitatively, that the CNN-LSTM-RF ensemble proposed gives genuinely superior fault classification performance compared with the baselines tested, as opposed to marginal improvements or spuriously measured improvements.

5.4 CRITICAL ANALYSIS AND COMPARISON WITH PRIOR WORK

The model proposed achieves an overall classification accuracy of 98.76% on operational PMU data as compared to all previous empirical benchmarks on real-world datasets for further improvement within the field. The closest comparison of which we are aware in the literature using operational (not simulated) data is that of Guo et al. A three-layer LSTM and published [26] where performance has reached96.8% on8400 operational PMU records, representing a 1.96 percentage point performance gap. Although this result may seem modest, it amounts to a 58.7% error reduction in fault misclassification rate overGuo et al. (1.24% vs 3.20% misclassification rate) a practically significant reduction in a protection context where any misidentification can either cause an incorrect relay operation or postpone fault clearance. The performance of the proposed model reaches near-parity with 98.4% for simulation-based benchmarks reported by Dong et al [28] by employing Transformer architectures on synthetic data with orders of magnitude lower inference latency (8.3 ms vs. 31.7 ms for the Transformer model) a critical operational benefit for time-sensitive relay decision support statement

The 96.98% F1-score in classifying high-impedance faults deserves special critical attention. Santoso et al. Using wavelet energy features, HIF was classified with an accuracy of 91.2% (reported in [17]) and Samantaray et al. Simulated Data with Idealized Noise Profiles 93.4% SVM Accuracy for HIF Both [20] Nevertheless the current model score of 96.98% on operational data with realistic noise is a significant step forward, due to the fact that the LSTM can now better track HIF events over time windows orders of magnitude larger than any single-cycle analysis window possible using conventional relay algorithms, since the pattern of intermittent, non-stationary current injection from arcing HIFs signals develops slowly and evolves over cycles. There remains the puzzle of 1.7% confusion between HIF and SLG-A that must be unravelled. Confusion case analysis shows that most confusions happen during HIF with impedance values ranging between 60 and 80 Ω and at fault distances between 15–25% from the PMU, where magnitudes of fault current temporarily fall within the SLG-A current magnitude range for certain ranges of fault inception angles. This impedance-distance-angle confound is a commonly acknowledged drawback of data-driven classifiers and hints that physics-informed constraints (e.g. explicit fault impedance estimation from sequence component ratios as a pre-classification feature) could further minimize inter-class confusion for these edge cases.

The low latency of the 8.3 ms on-device inference speed of k-NN based fault direction identification is greatly satisfies the < 10 ms requirement of IEC 61850 Zone 1 protection application for high-speed fault clearance applications while 18.7 ms and 31.7 ms of latency with k-NN and Transformer respectively kh468f is observed from They matched Rockwell Automation model evaluation includes a test to measure suitability to run on embedded edge processing platforms while satisfying microsecond-level processing requirement in real-time IED-based industrial smart grid information models[14]. With only a 5.2 ms latency overhead (relative to SVM's 3.1 ms), this yields an operationally acceptable trade-off given the quality of protection improvement delivered (+4.2% relative accuracy over SVM, the most broadly deployed ML method in contemporary operational protection relays). In contrast to the wavelet-SVM hybrid approaches which comprise majority of recent literature, the end-to-end deep learning approach avoids hyperparameter sensitivity regarding selection of wavelet decomposition level and does not require manual feature engineering thus decreasing system development/maintenance overhead in an operational deployment context. Together, these benefits along with the statistical significance demonstrated in both the ANOVA and Cohen's d analysis substantiate the proposed method as a candidate for implementation within next-generation digital substation architectures compliant to IEC 61850 and IEC 61968/61970 Common Information Model standards.

6. CONCLUSION

In this paper we have conducted a thorough empirical study of AI-enabled fault detection and classification for high-voltage transmission lines based on real-time PMU data gathered from an operational national grid. The proposed hybrid CNN-LSTM-Random Forest ensemble trained and evaluated on the dataset of 52,800 fault records generated from fourteen PMU substations operated in the Indian Northern Regional Grid is capable of classifying faults with an accuracy equal to 98.76 ± 0.31%, F1-score equal to 98.61% and Area Under Curve-

Receiver Operating Characteristic (AUC-ROC) equal here to AUC-IR=0.9974 over ten fault categories. The model meets the IEC 61850 real-time protection requirement with an inference latency of 8.3 ms using edge deployment hardware. The statistical significance and large practical effectiveness of this performance advantage is statistically validated using one-way ANOVA ($F = 142.67$, $p < 0.001$), Tukey HSD post-hoc testing and effect size analysis (Cohen's d) over a total of six fellow competitive baselines: SVM, k-NN, Naive Bayes and Decision Tree classifiers.

Results show that the deep learning architectures with convolutional spatial feature extraction, recurrent temporal modeling, and probabilistic ensemble refinement provide a robust characterization of fault dynamics even in operational PHM environments subject to significant measurement noise, GPS synchronization artifacts and multi-fault topology complexities. The remaining 96.98% F1-score for high-impedance faults indicates a future research direction where physics-informed features are automatically extracted from sequence component impedance trajectories. This framework should be a foundation for future studies to include online continual learning approaches where the model can adjust based on increasingly utilized grid topology and loading conditions, as well as federated learning architectures that allow for models to simultaneously train across utilities of data without requiring the sharing of sensitive operational details with other entities (George et al., 20163). The deployment guidelines and statistical validation methodology presented in this study are suggested as a reproducible template for the benefit of utility engineers and researchers interested in deploying AI-based protection intelligence within smart grid structures throughout the world.

REFERENCES

1. Rahman, M. S., Bin Romlie, M. F., Binti Md Hasan, K. N., Bin Abdullah, M. F., & Bin Ibrahim, T. (2026). Unintentional islanding detection in electrical power distribution systems via PMU and a classification-enabled machine learning algorithm. *Electrical Engineering*, *108*(2), 81.

2. Daggupati, V., & Jammula, S. N. S. (2026). Recent advances in fault diagnosis techniques for high voltage transmission lines: A review. *Recent Advances in Fault Diagnosis Techniques for High*, *6*(02), 284-292.

3. Bin Akter, S., Pias, T. S., Deeba, S. R., Hossain, J., Rahman, H. A., Donta, P. K. (2024). Ensemble learning based transmission line fault classification using phasor measurement unit (PMU) data with explainable AI (XAI). *PLOS ONE*, *19*(2), e0295144. https://doi.org/10.1371/journal.pone.0295144

4. Kusuma, H. (2024). Deep learning-based disturbance detection in smart distribution networks using PMU data. *Elimensi: Journal of Electrical Engineering*, *2*(01), 28–33. https://doi.org/10.62381/elimensi.v2i01.428

5. Alhanaf, A. S., Farsadi, M., & Balik, H. H. (2024). Fault detection and classification in ring power system with DG penetration using hybrid CNN-LSTM. *IEEE Access*, *12*, 59953–59975. https://doi.org/10.1109/ACCESS.2024.3394166

6. Yousaf, M. Z., Ali, S., Akhtar, M., & Haider, A. (2024). Bayesian-optimized LSTM-DWT approach for reliable fault detection in MMC-based HVDC systems. *Scientific Reports*, *14*(1), 17968. https://doi.org/10.1038/s41598-024-68985-5

7. Thomas, J. B., Chaudhari, S. G., Verma, N. K. (2023). CNN-based transformer model for fault detection in power system networks. *IEEE Transactions on Instrumentation and Measurement*, *72*, 1–10. https://doi.org/10.1109/TIM.2022.3219759

8. Shadi, M. R., Ameli, M. T., & Azad, S. (2022). A real-time hierarchical framework for fault detection, classification, and location in power systems using PMUs data and deep learning. *International Journal of Electrical Power & Energy Systems*, *134*, 107399. https://doi.org/10.1016/j.ijepes.2021.107399

9. Alqudah, M., Pavlovski, M., Dokic, T., Kezunovic, M., Hu, Y., & Obradovic, Z. (2022). Fault detection utilizing convolution neural network on timeseries synchrophasor data from phasor measurement units. *IEEE Transactions on Power Systems*, *37*(5), 3434–3442. https://doi.org/10.1109/TPWRS.2021.3135336

10. Moradzadeh, A., Teimourzadeh, H., Mohammadi-Ivatloo, B., & Pourhossein, K. (2022). Hybrid CNN-LSTM approaches for identification of type and locations of transmission line faults. *International Journal of Electrical Power & Energy Systems*, *135*, 107563. https://doi.org/10.1016/j.ijepes.2021.107563

11. Otudi, H., Dokic, T., Mohamed, T., Kezunovic, M., Hu, Y., & Obradovic, Z. (2022). Line faults classification using machine learning on three phase voltages extracted from large dataset of PMU measurements. *Proceedings of the 55th Hawaii International Conference on System Sciences*. https://doi.org/10.24251/hicss.2022.425

12. Shi, J., Yamashita, K., & Yu, N. (2022). Power system event identification with transfer learning using large-scale real-world synchrophasor data. *2022 IEEE Power & Energy Society Innovative Smart Grid Technologies Conference (ISGT)*. https://doi.org/10.1109/ISGT50606.2022.9817516

13. Fahim, S. R., Sarker, S. K., Muyeen, S. M., Das, S. K., & Kamwa, I. (2021). A deep learning based intelligent approach in detection and classification of transmission line faults. *International Journal of Electrical Power & Energy Systems*, *133*, 107102. https://doi.org/10.1016/j.ijepes.2021.107102

14. Belagoune, S., Bali, N., Bakdi, A., Baadji, B., & Atif, K. (2021). Deep learning through LSTM classification and regression for transmission line fault detection, diagnosis and location in large-scale multi-machine power systems. *Measurement*, *177*, 109330. https://doi.org/10.1016/j.measurement.2021.109330

15. Li, Z., Shahidehpour, M., Alabdulwahab, A., & Abusorrah, A. (2021). A power system disturbance classification method robust to PMU data quality issues. *IEEE Transactions on Industrial Informatics*, *18*(1), 130–142. https://doi.org/10.1109/TII.2021.3073719

16. Swain, K., & Cherukuri, M. (2021). Intelligent fault analysis of transmission line using phasor measurement unit incorporating auto-reclosure protection scheme. *SN Applied Sciences*, *3*, 531. https://doi.org/10.1007/s42452-021-04510-x

17. Pavlovski, M., Alqudah, M., Dokic, T., Abdel Hai, A., Kezunovic, M., & Obradovic, Z. (2021). Hierarchical convolutional neural networks for event classification on PMU data. *IEEE Transactions on Instrumentation and Measurement*, *70*, 1–13. https://doi.org/10.1109/TIM.2021.3115583

18. Wu, H., Wang, Q., Yu, K., Hu, X., & Ran, M. (2020). A novel intelligent fault identification method based on random forests for HVDC transmission lines. *PLOS ONE*, *15*(3), e0230717. https://doi.org/10.1371/journal.pone.0230717

19. Wang, W., Guan, L., Chen, Y., & Zhang, J. (2020). Frequency disturbance event detection based on synchrophasors and deep learning. *IEEE Transactions on Smart Grid*, *11*(4), 3593–3605. https://doi.org/10.1109/TSG.2020.2975431

20. Swain, K. B., Mahato, S. S., & Cherukuri, M. (2019). Expeditious situational awareness-based transmission line fault classification and prediction using synchronized phasor measurements. *IEEE Access*, *7*, 168187–168200. https://doi.org/10.1109/ACCESS.2019.2954337

21. Li, W., Deka, D., Chertkov, M., & Wang, M. (2019). Real-time faulted line localization and PMU placement in power systems through convolutional neural networks. *IEEE Transactions on Power Systems*, *34*(6), 4640–4651. https://doi.org/10.1109/TPWRS.2019.2917794

22. Porwal, R. K., Swarup, K. S., & Thomas, M. S. (2019). Analysis of effectiveness of PMU based wide area monitoring system in Indian power grid. *2018 IEEE International Conference on Power Electronics, Drives and Energy Systems (PEDES)*. https://doi.org/10.1109/PEDES.2018.8596838

23. Zhang, S., Wang, Y., Liu, M., & Bao, Z. (2017). Data-based line trip fault prediction in power systems using LSTM networks and SVM. *IEEE Access*, *6*, 7675–7686. https://doi.org/10.1109/ACCESS.2017.2785763

24. Aftab, M. A., Hussain, S. M. S., Ali, I., & Ustun, T. S. (2020). IEC 61850 based substation automation system: A survey. *International Journal of Electrical Power and Energy Systems*, *120*, 106008. https://doi.org/10.1016/j.ijepes.2020.106008

25. Ghaderi, A., Ginn, H. L., & Mohammadpour, H. A. (2017). High impedance fault detection: A review. *Electric Power Systems Research*, *143*, 376–388. https://doi.org/10.1016/j.epsr.2016.10.031

26. Rai, P., Singh, S., & Rathore, A. (2021). Application of machine learning methods in fault detection and classification of power transmission lines: A survey. *Artificial Intelligence Review*, *56*, 2697–2738. https://doi.org/10.1007/s10462-022-10296-0

27. Rafique, F., Fu, L., & Mai, R. (2021). End to end machine learning for fault detection and classification in power transmission lines. *Electric Power Systems Research*, *199*, 107430. https://doi.org/10.1016/j.epsr.2021.107430

28. Wang, X., Zhou, P., Peng, X., Wu, Z., & Yuan, H. (2022). Fault location of transmission line based on CNN-LSTM double-ended combined model. *Energy Reports*, *8*, 781–791. https://doi.org/10.1016/j.egyr.2021.11.248

29. Dusabimana, E., & Yoon, S. G. (2020). A survey on the micro-phasor measurement unit in distribution networks. *Electronics*, *9*(2), 305. https://doi.org/10.3390/electronics9020305

30. Samantaray, S. R., Dash, P. K., & Upadhyay, S. K. (2010). Adaptive Kalman filter based fault detector and classifier for transmission lines in distributed generation system. *International Journal of Electrical Power & Energy Systems*, *32*(6), 620–629. https://doi.org/10.1016/j.ijepes.2009.11.025

31. Dash, P. K., Samantaray, S. R., & Panda, G. (2007). Fault classification and section identification of an advanced series-compensated transmission line using support vector machine. *IEEE Transactions on Power Delivery*, *22*(1), 67–73. https://doi.org/10.1109/TPWRD.2006.876695

32. Santoso, S., Powers, E. J., Grady, W. M., & Hofmann, P. (2010). Wavelet transform-based analysis of electric power quality disturbances. In *Power Quality in Power Systems and Electrical Machines* (2nd ed., pp. 249–295). Academic Press. https://doi.org/10.1016/B978-0-12-369536-9.00007-1